Frequency-domain theory of nonsequential double ionization in intense laser fields based on nonperturbative QED

Bingbing Wang,[1,*] Yingchun Guo,[2] Jing Chen,[3,4] Zong-Chao Yan,[5] and Panming Fu[1]

[1]*Laboratory of Optical Physics, Beijing National Laboratory for Condensed Matter Physics, Institute of Physics, Chinese Academy of Sciences, Beijing 100190, China*

[2]*State Key Laboratory of Precision Spectroscopy, Department of Physics, East China Normal University, Shanghai 200062, China*

[3]*Key Laboratory of High Energy Density Physics Simulation, CAPT, Peking University, Beijing 100084, China*

[4]*Institute of Applied Physics and Computational Mathematics, P.O. Box 8009, Beijing 100088, China*

[5]*Department of Physics, University of New Brunswick, Fredericton, New Brunswick, Canada E3B 5A3*

(Received 1 November 2011; published 2 February 2012)

We study nonsequential double ionization (NSDI) processes of an atom by applying the frequency-domain theory based on the nonperturbative quantum electrodynamics. We obtain the transition formulas that describe the NSDI processes caused by the collision ionization (CI) and the collision-excitation ionization (CEI) mechanisms. By analyzing the NSDI results of each above-threshold ionization (ATI) channel, we investigate the contributions to the NSDI from the backward and forward collisions. In particular, for the CI process, the backward collision makes a major contribution to the NSDI probability, whereas for the CEI process, it depends on the characteristics of the laser-atom system: if the energy that the recolliding electron needs to excite a bound electron is much larger than the laser photon energy, such as for the case of helium in this work, the backward collision dominates the contribution; otherwise, the forward collision dominates the contribution. We also discuss the source of interference fringes in the NSDI momentum spectra due to the CI mechanism and find that the fringes can be predicted by using a simple cosine function. This work can be regarded as a development of the frequency-domain theory, which may shed light on the study of multiparticle dynamics in intense laser fields.

DOI: 10.1103/PhysRevA.85.023402 PACS number(s): 32.80.Rm, 42.65.−k, 42.50.Hz

I. INTRODUCTION

A recollision process of an electron in a strong laser field [1], such as high-order harmonic generation (HHG), high-order above-threshold ionization (HATI), and nonsequential double ionization (NSDI), provides us with a window to do in-depth study on the interaction between matter and the intense laser field [2] and also with the possibility to control the corresponding highly nonlinear transition process [3]. For example, HHG can be used to obtain ultrashort attosecond pulses [4,5] and to image atomic or molecular structures [6–10], HATI can be used to investigate molecular structures [11–15] and dynamics [16], and NSDI shows that the multielectron ionization in an intense laser field is not always sequentially one by one [17–22]. It is often the case that these three phenomena, i.e., HHG, HATI, and NSDI, may occur during a single recollision process, implying that we may treat them under a unified theoretical frame. One such approach is the frequency-domain theory based on the nonperturbative quantum electrodynamics (QED) [23], which has recently been developed to deal with recollision processes [13,15,24–27], including HHG and HATI. By using this theory, Fu *et al.* [25] have investigated the relationship between ATI and HHG and found that the origin of the plateau on a HHG spectrum is attributed to a laser-assisted recombination process. Recently, Guo *et al.* [13] have investigated the interference fringes in the HATI spectra of molecules and found the charge distribution effect of imaging the molecular structure by HATI [15].

With the help of formal scattering theory [28], the frequency-domain theory provides a different viewpoint on the interaction between matter and the intense laser field. In this theory, all dynamic processes can be treated as quantum transitions between two states of a laser-matter system, where the laser field, as a part of the whole system, is treated as a quantized field. Based on this theory, a recollision can be considered as a two-step process: an above-threshold ionization (ATI), followed by a laser-assisted collision (LAC) or a laser-assisted recombination (LAR). Consequently, the characteristics of a recollision process lay in the LAC or LAR, with a weight given by the first-step ATI transition. For example, the quantum interference fringes in an angle-resolved HATI spectrum of a diatomic molecule are attributable to the two-center LAC and the oscillation of recolliding electrons driven by the laser [13]. In this paper, we will develop this method to investigate the NSDI process. By analyzing the contributions of each ATI channel to NSDI, we investigate the source of interference fringes in NSDI momentum spectra as well as the contributions of backward and forward collisions. In particular, we find that the backward collision dominates the contribution to NSDI for the collision ionization mechanism, whereas the contributions of the backward and forward collisions to NSDI for the collision-excitation ionization mechanisms depend on the characteristics of the laser-atom system. All these results can be interpreted by looking at the corresponding Bessel functions involved in the LAC process.

This paper is organized as follows. In Sec. II, we describe the frequency-domain theory of NSDI. In Sec. III, we investigate the NSDI contributed by the collision ionization mechanism and discuss the source of quantum interference in a two-electron momentum spectrum. In Sec. IV, we present the NSDI results due to the collision-excitation ionization mechanism for low laser intensities. Finally, in Sec. V, we make our conclusions.

*wbb@aphy.iphy.ac.cn.

II. FREQUENCY-DOMAIN THEORY OF NSDI

The Hamiltonian for a two-electron atom interacting with a single-mode laser field is [29]

$$H = H_0 + U + V. \tag{1}$$

In the above expression (atomic units are used throughout unless otherwise stated),

$$H_0 = \frac{(-i\nabla_1)^2}{2} + \frac{(-i\nabla_2)^2}{2} + \omega N_a \tag{2}$$

is the free electron and photon energy operator and $N_a = (a^\dagger a + aa^\dagger)/2$ is the photon number operator, with a ($a^\dagger$) being the annihilation (creation) operator of the laser photon mode. Also, $U = U_1 + U_2 + U_{12}$, where U_1 and U_2 are the interaction potentials between the nucleus and the two electrons, respectively, and U_{12} is the interaction potential between the two electrons. Finally, the electron-photon interaction potential is $V = V_1 + V_2$, where

$$V_j = -\mathbf{A}(\mathbf{r}_j)\cdot(-i\nabla_j) + \frac{\mathbf{A}^2(\mathbf{r}_j)}{2}, \quad j = 1,2, \tag{3}$$

$\mathbf{A}(\mathbf{r}_j) = g(\hat{\varepsilon}ae^{i\mathbf{k}\cdot\mathbf{r}_j} + \text{c.c.})$ is the vector potential, $g = (2\omega V_\gamma)^{-1/2}$, $\mathbf{k}$ is the wave vector, V_γ is the normalization volume of the photon modes, and $\hat{\varepsilon} = \hat{z}$ is the polarization vector of the laser mode.

The frequency-domain theory based on the above-mentioned Hamiltonian enables us to treat an atom-laser interaction process as a genuine scattering process in an isolated system that consists of an atom and a laser field. Since the total energy of the system is conserved throughout the interaction process, the formal scattering theory [28] thus applies. The NSDI process is a transition from an initial two-electron bound state with U being on and V being off to a final two-electron Volkov state with V being on and U being off. It is assumed that the interaction-free initial state ψ_i satisfies $(H_0 + U)\psi_i = E_i\psi_i$ and the final state ψ_f of the free electrons in the laser field satisfies $(H_0 + V)\psi_f = E_f\psi_f$. Then the scattering wave function for the initial state can be written as [28]

$$\psi_i^+ = \psi_i + \frac{1}{E_i - H + i\epsilon}V\psi_i, \tag{4}$$

and the scattering wave function for the final state is

$$\psi_f^- = \psi_f + \frac{1}{E_f - H' - i\epsilon}U\psi_f + \frac{1}{E_f - H' - i\epsilon}U\frac{1}{E_f - H - i\epsilon}V\psi_f, \tag{5}$$

with $H' = H_0 + U$. The S matrix for the transition from ψ_i to ψ_f is

$$S_{fi} = \delta_{fi} - 2\pi i\delta(E_f - E_i)T_{fi}, \tag{6}$$

where the T matrix element can be written as

$$\begin{aligned} T_{fi} = \langle\psi_f|\left[U + V\frac{1}{E_f - H - i\epsilon}U\right]|\psi_i^+\rangle &= \langle\psi_f|U|\psi_i\rangle + \langle\psi_f|V\frac{1}{E_f - H - i\epsilon}U|\psi_i\rangle \\ &+ \langle\psi_f|U\frac{1}{E_i - H + i\epsilon}V|\psi_i\rangle + \langle\psi_f|V\frac{1}{E_f - H - i\epsilon}U\frac{1}{E_i - H + i\epsilon}V|\psi_i\rangle. \end{aligned} \tag{7}$$

The first term in Eq. (7) can be rewritten as $\langle\psi_f|U|\psi_i\rangle = \langle\psi_f|E_i - H_0|\psi_i\rangle$. Since the total energy of the system is constant during the transition process, i.e., $E_f = E_i$, we have $\langle\psi_f|U|\psi_i\rangle = \langle\psi_f|E_f - H_0|\psi_i\rangle = \langle\psi_f|V|\psi_i\rangle$.

Since the T matrix includes many quantum paths leading to a double ionization of the two electrons, we should now classify these transition paths according to the components of the T matrix as follows:

$$T_{fi} = T_0 + T_1 + T_2, \tag{8}$$

where

$$T_0 = \langle\psi_f|V|\psi_i\rangle, \tag{9}$$

$$T_1 = \langle\psi_f|V\frac{1}{E_f - H - i\epsilon}U|\psi_i\rangle + \langle\psi_f|U\frac{1}{E_i - H + i\epsilon}V|\psi_i\rangle, \tag{10}$$

$$T_2 = \langle\psi_f|V\frac{1}{E_f - H - i\epsilon}U\frac{1}{E_i - H + i\epsilon}V|\psi_i\rangle. \tag{11}$$

Substituting $V = V_1 + V_2$ and $U = U_1 + U_2 + U_{12}$ into Eqs. (9)–(11), the transition paths can be classified as follows: (1) T_0 corresponds to the process where one electron is ionized by the laser field and the other electron is shaken off. (2) T_1 includes three subpaths: (2a) one electron is ionized and then recollides with the core, and the other electron is shaken off ($V_1 \dashrightarrow U_1$); (2b) one electron is ionized by the laser field, and the other electron is shaken off and then recollides with the core ($V_1 \dashrightarrow U_2$); (2c) one electron is ionized, and then it recollides with the other electron and sets the other one free via the collision ($V_1 \dashrightarrow U_{12}$). (3) T_2 includes six subpaths: (3a) one electron e_1 is ionized by the laser field and then

recollides with the core, resulting in being captured by the core; finally, it is ionized by the laser again, whereas the other electron e_2 is shaken off ($V_1 \dashrightarrow U_1 \dashrightarrow V_1$). (3b) One electron e_1 is excited by the laser field, and the second electron e_2 is shaken off; then e_2 recollides with the core, and finally, e_1 is ionized by the laser field ($V_1 \dashrightarrow U_2 \dashrightarrow V_1$). (3c) One electron e_1 is ionized by the laser field and recollides with the other electron e_2; then e_2 is ionized by the collision, but e_1 is captured by the core; finally, e_1 is ionized by the laser field again ($V_1 \dashrightarrow U_{12} \dashrightarrow V_1$). (3d) One electron e_1 is ionized by the laser field, and then it recollides with the core; the other electron e_2 is then ionized by the laser field ($V_1 \dashrightarrow U_1 \dashrightarrow V_2$). (3e) One electron e_1 is ionized by the laser field, and the other electron e_2 is shaken off; then e_2 recollides with the core and is recaptured by the core, and finally, e_2 is ionized by the laser field ($V_1 \dashrightarrow U_2 \dashrightarrow V_2$). (3f) One electron e_1 is ionized by the laser field, and then it recollides with the other electron e_2 and excites it; finally, the excited electron e_2 is ionized by the laser field ($V_1 \dashrightarrow U_{12} \dashrightarrow V_2$).

Among the above-mentioned transition paths, path (2c), which represents the collision-ionization (CI) process, and path (3f), which represents the collision-excitation-ionization (CEI) process, are proven to have major contributions to NSDI under the current low-frequency laser conditions [19]. In the following, we will focus on these two paths. The transition term for CI is

$$T_{\rm CI} = \langle \psi_f \mid U_{12} \frac{1}{E_i - H + i\epsilon} V_1 \mid \psi_i \rangle , \tag{12}$$

and the transition term of CEI is

$$T_{\rm CEI} = \langle \psi_f \mid V_2 \frac{1}{E_f - H - i\epsilon} U_{12} \frac{1}{E_i - H + i\epsilon} V_1 \mid \psi_i \rangle . \tag{13}$$

The initial state of the atom-laser system is $\mid \psi_i \rangle = \mid \Phi_i(\mathbf{r}_1,\mathbf{r}_2), n_i \rangle = \Phi_i(\mathbf{r}_1,\mathbf{r}_2) \otimes \mid n_i \rangle$, which is the eigenstate of the Hamiltonian $H_0 + U(\mathbf{r}_1,\mathbf{r}_2)$ with the energy $E_i = -E_{12} + (n_i + \frac{1}{2})\omega$. Here $\Phi_i(\mathbf{r}_1,\mathbf{r}_2)$ is the ground state of He, with E_{12} being the ionization energy of this state, and $\mid n_i \rangle$ is the Fock state of the laser mode with the photon number n_i. On the other hand, the final state $\mid \psi_f \rangle = \Psi_{\mathbf{p}_1\mathbf{p}_2 k}$, with the energy $E_f = E_{\mathbf{p}_1\mathbf{p}_2 k}$ being the quantized-field Volkov state with two electrons in a single laser field [30],

$$\begin{aligned} \Psi_{\mathbf{p}_1\mathbf{p}_2 k} = V_e^{-1} \sum_{j_1=-k}^{\infty} & \exp\{i[\mathbf{p}_1 + (u_p - j_1)\mathbf{k}] \cdot \mathbf{r}_1\} \mathcal{J}_{j_1}(\zeta_1,\eta)^* \\ \times \sum_{j_2=-k-j_1}^{\infty} & \exp\{i[\mathbf{p}_2 + (u_p - j_2)\mathbf{k}] \cdot \mathbf{r}_2\} \mathcal{J}_{j_2}(\zeta_2,\eta)^* \\ \times & \mid k + j_1 + j_2 \rangle, \end{aligned} \tag{14}$$

which is an ansatz from the general one-electron Volkov state [23] by assuming that the two electrons are separated far away from each other so that the correlation between them can be ignored. Also in the above V_e is the normalization volume for the free electrons, $u_p = \Lambda^2/\omega$ is the ponderomotive energy in units of the photon energy in the laser, and $\Lambda = g\sqrt{k}$ gives the half amplitude of the classical field in the limit of $g \to 0$ and $k \to \infty$. The integer j_i, with $i = 1$ or 2, represents the photon number transferred between the laser field and one of the electrons. The generalized Bessel function $\mathcal{J}_{j_i}(\zeta_i,\eta)$, with $i = 1$ or 2, is defined in terms of the ordinary Bessel functions as $\mathcal{J}_{j_i}(\zeta_i,\eta) = \sum_{m=-\infty}^{\infty} J_{-j_i-2m}(\zeta_i) J_m(\eta)$, where $\zeta_i = (2\Lambda/\omega)\mathbf{p}_i \cdot \hat{\epsilon}$, with $\mathbf{p}_i$ being the momentum of the corresponding electron and $\eta = u_p/2$ [23]. We should notice that the final state Eq. (14) for the two ionized electrons does not include the Coulomb interaction between these two ionized electrons. Therefore the so-called "finger-like" structure in the correlated electron momentum distribution shown in Refs. [31,32] is not expected to appear in our results. This approximation may be improved by including the Coulomb interaction between the two ionized electrons in future work.

In the first step in a NSDI transition, an electron in helium is ionized, and the other electron is still bounded. Therefore, an intermediate state can be expressed as $\Psi_{\mathbf{p}_1 m} \otimes \Phi_1(\mathbf{r}_2)$, where $\Phi_1(\mathbf{r}_2)$ is the ground state of He^+. Also, $\Psi_{\mathbf{p}_1 m}$ is the well-known Volkov state,

$$\begin{aligned} \Psi_{\mathbf{p}_1 m} = V_e^{-1/2} \sum_{j=-m}^{\infty} & \exp\{i[\mathbf{p}_1 + (u_p - j)\mathbf{k}] \cdot \mathbf{r}_1\} \\ & \times \mathcal{J}_j(\zeta_1,\eta)^* \mid m + j \rangle. \end{aligned} \tag{15}$$

By using the completeness relation of the intermediate states together with the initial and final states, we can express the CI transition term as

$$\begin{aligned} T_{\rm CI} = -i\pi \sum_{\mathbf{p}'_1 m} & \langle \Psi_{\mathbf{p}_1\mathbf{p}_2 k} \mid U_{12} \mid \psi_{\mathbf{p}'_1 m} \Phi_1(\mathbf{r}_2) \rangle \langle \Psi_{\mathbf{p}'_1 m} \Phi_1(\mathbf{r}_2) \mid \\ & \times V_1 \mid \Phi_i, n_i \rangle \delta\big(E_f - E_{\mathbf{p}'_1 m}\big). \end{aligned} \tag{16}$$

On the other hand, for a CEI process, we need another set of intermediate states where the bound electron is in its excited state. In our calculation, we found that the NSDI yield contributed by the first excited state is more than three orders of magnitude larger than that contributed by the second excited states. Hence we only consider the first excited state of the bound electron, and then an intermediate state in this set can be expressed as $\Psi_{\mathbf{p}''_1 l} \otimes \Phi_2(\mathbf{r}_2)$, with $\Phi_2(\mathbf{r}_2)$ being the first excited state of He^+ and $\Psi_{\mathbf{p}''_1 l}$ being the Volkov state of the ionized electron in the laser field after it recollides with the bound electron. Thus the CEI transition term can be written as

$$\begin{aligned} T_{\rm CEI} = \pi^2 \sum_{\mathbf{p}''_1 l} \sum_{\mathbf{p}'_1 m} & \langle \Psi_{\mathbf{p}_1\mathbf{p}_2 k} \mid V_2 \mid \psi_{\mathbf{p}''_1 l} \Phi_2(\mathbf{r}_2) \rangle \langle \Psi_{\mathbf{p}''_1 l} \Phi_2(\mathbf{r}_2) \mid \\ & \times U_{12} \mid \psi_{\mathbf{p}'_1 m} \Phi_1(\mathbf{r}_2) \rangle \langle \Psi_{\mathbf{p}'_1 m} \Phi_1(\mathbf{r}_2) \mid V_1 \mid \Phi_i, n_i \rangle \\ & \times \delta\big(E_f - E_{\mathbf{p}''_1 l}\big) \delta\big(E_{\mathbf{p}''_1 l} - E_{\mathbf{p}'_1 m}\big). \end{aligned} \tag{17}$$

The physics underlying Eqs. (16) and (17) can be understood as follows. The transition term $\langle \Psi_{\mathbf{p}'_1 m} \Phi_1(\mathbf{r}_2) \mid V_1 \mid \Phi_i, n_i \rangle$ in both Eqs. (16) and (17) represents the direct ATI amplitude of the first electron e_1, where it absorbs $j = n_i - m$ photons from the laser field and is ionized with momentum $\mathbf{p}'_1$. Furthermore, the term $\langle \Psi_{\mathbf{p}_1\mathbf{p}_2 k} \mid U_{12} \mid \psi_{\mathbf{p}'_1 m} \Phi_1(\mathbf{r}_2) \rangle$ in Eq. (16) represents the laser-assisted collision ionization (LACI) of the bound electron e_2, where the first ionized electron collides with the bound electron and sets it free from the ground state of He^+ ion under the help of the laser field by absorbing $m - k$ photons; the term $\langle \Psi_{\mathbf{p}''_1 l} \Phi_2(\mathbf{r}_2) \mid U_{12} \mid \psi_{\mathbf{p}'_1 m} \Phi_1(\mathbf{r}_2) \rangle$ in Eq. (17) is the amplitude of the laser-assisted collision excitation

(LACE) of the bound election e_2 by the collision of the first electron, followed by the term $\langle \Psi_{\mathbf{p}_1\mathbf{p}_2 k} \mid V_2 \mid \psi_{\mathbf{p}_1'' l} \Phi_2(\mathbf{r}_2)\rangle$, which is the direct ATI transition of e_2 from its excited state. Additionally, since the first electron has no relationship with the ATI process of e_2, it keeps its momentum during the ATI process of e_2, i.e., $\mathbf{p}_1'' = \mathbf{p}_1$.

The ATI transition matrix element $\langle \Psi_{\mathbf{p}_1' m} \Phi_1(\mathbf{r}_2) \mid V_1 \mid \Phi_i, n_i \rangle$ can be written as [23]

$$\langle \Psi_{\mathbf{p}_1' m} \Phi_1(\mathbf{r}_2) | V_1 | \Phi_i, n_i \rangle = V_e^{-1/2} \omega(u_p - j) \Phi'(p_1') \mathcal{J}_j(\zeta_1', \eta), \tag{18}$$

where $j = n_i - m$, $\zeta_1' = (2\Lambda\omega)\mathbf{p}_1' \cdot \hat{\epsilon}$, $\mathbf{p}_1'$ is the momentum of the first ionized electron before recollision and $\Phi'(p_1') = \iint d\mathbf{r}_1 d\mathbf{r}_2 \exp[-i\mathbf{p}_1' \cdot \mathbf{r}_1] \Phi_1(\mathbf{r}_2) \Phi_i(\mathbf{r}_1, \mathbf{r}_2)$. In order to simplify the actual calculation of $\Phi'(p_1')$, here we make an approximation that the ground-state wave function is a product of two one-electron ground-state wave functions and the second electron remains in its initial state when the first electron is ionized [33,34]. At present, the influence of this approximation of the initial state on the final NSDI results is still an open question. Then the LACI transition matrix element becomes

$$\begin{aligned} &\langle \Psi_{\mathbf{p}_1\mathbf{p}_2 k} | U_{12} | \psi_{\mathbf{p}_1' m} \Phi_1(\mathbf{r}_2) \rangle \\ &\quad = V_e^{-3/2} \sum_j \sum_{j'} I(\mathcal{P}) \mathcal{J}_{j_1}(\zeta_1, \eta) \mathcal{J}_{m + j_1' - k - j_1} \\ &\qquad \times (\zeta_2, \eta) \mathcal{J}^*_{j_1'}(\zeta_1', \eta), \end{aligned} \tag{19}$$

where

$$\begin{aligned} I(\mathcal{P}) = \iint d\mathbf{r}_1 d\mathbf{r}_2 \exp[-i(\mathbf{p}_1 - \mathbf{p}_1') \cdot \mathbf{r}_1] \\ \times \exp[-i\mathbf{p}_2 \cdot \mathbf{r}_2] U_{12} \Phi_1(\mathbf{r}_2) \end{aligned} \tag{20}$$

is the coordinate integral due to the collision-ionization process, with $\mathbf{p}_1$ and $\mathbf{p}_2$ being the final momenta of the two ionized electrons, and $\mathcal{P}$ denotes $(\mathbf{p}_1, \mathbf{p}_2, \mathbf{p}_1')$. Consequently, by using Eqs. (18) and (19), the CI transition matrix term T_{CI} can be written as

$$\begin{aligned} T_{\mathrm{CI}} = -i\pi V_e^{-2} \sum_{\mathbf{p}_1', s} I(\mathcal{P}) \mathcal{J}_{q_1 + q_2 - s}(\zeta_1 + \zeta_2 - \zeta_1', \eta) \\ \times \omega(u_p - s) \Phi'(p_1)' \mathcal{J}_s(\zeta_1', \eta) \delta\big(E_f - E_{\mathbf{p}_1' m}\big). \end{aligned} \tag{21}$$

We notice that Eq. (21) agrees with the formula obtained by Becker and Faisal from their Feynman-like diagram approach [19].

On the other hand, the LACE transition matrix element can be written as

$$\langle \Psi_{\mathbf{p}_1 l} \Phi_2(\mathbf{r}_2) | U_{12} | \psi_{\mathbf{p}_1' m} \Phi_1(\mathbf{r}_2) \rangle = V_e^{-1} I'(\mathcal{P}) J_{m-l}(\zeta_1 - \zeta_1'), \tag{22}$$

where $J_{m-l}(\zeta_1 - \zeta_1')$ is an ordinary Bessel function and

$$I'(\mathcal{P}) = \iint d\mathbf{r}_1 d\mathbf{r}_2 \exp[-i(\mathbf{p}_1 - \mathbf{p}_1') \cdot \mathbf{r}_1] U_{12} \Phi_1(\mathbf{r}_2) \Phi_2(\mathbf{r}_2), \tag{23}$$

with $\Phi_1(\mathbf{r}_2)$ and $\Phi_2(\mathbf{r}_2)$ being the ground and first excited states of He^+, respectively. Here $\mathcal{P}$ denotes $(\mathbf{p}_1, \mathbf{p}_1')$. Therefore, by using Eqs. (18) and (22), the CEI transition matrix term T_{CEI} can be expressed as

$$\begin{aligned} T_{\mathrm{CEI}} = \pi^2 V_e^{-2} \sum_{\mathbf{p}_1', s} I'(\mathcal{P}) J_{q_1 - s}(\zeta_1 - \zeta_1') \mathcal{J}_{q_2}(\zeta_2, \eta) \\ \times \omega^2 (u_p - s)(u_p - q_2) \Phi'(p_1') \Phi_2(p_2) \mathcal{J}_s(\zeta_1', \eta) \\ \times \delta\big(E_f - E_{\mathbf{p}_1 l}\big) \delta\big(E_{\mathbf{p}_1 l} - E_{\mathbf{p}_1' m}\big), \end{aligned} \tag{24}$$

where $\Phi_2(p_2)$ is the first excited state of He^+ in momentum space.

III. CHANNEL CONTRIBUTIONS AND QUANTUM INTERFERENCE IN A CI PROCESS

We now consider the NSDI probability by a CI process that is expressed by Eq. (21). Figure 1 presents the NSDI momentum spectra of two ionized electrons with their momenta along the polarization axis, as the laser intensity is 7×10^{14} W/cm^2. This result qualitatively agrees with the experimental results shown in Fig. 2(a) of Eremina *et al.* [35], where the corresponding perpendicular momenta have been integrated in their experiments. One may find that (1) the NSDI probability is dominated by processes where the final momenta of the two electrons are along the same directions (the first and third quadrants in Fig. 1), rather than along the opposite directions (the second and forth quadrants in Fig. 1), and (2) there are many interference fringes in Fig. 1, indicating that the NSDI process involves interference between quantum paths during a recollision. Now we would try to answer the following fundamental questions: At first, where does the quantum interference come from? Second, why is the NSDI probability dominated by the processes where the final momenta of two electrons are along the same direction, rather than in the opposite directions? Third, for the CI mechanism, which recollision process, the forward or backward, dominates the NSDI?

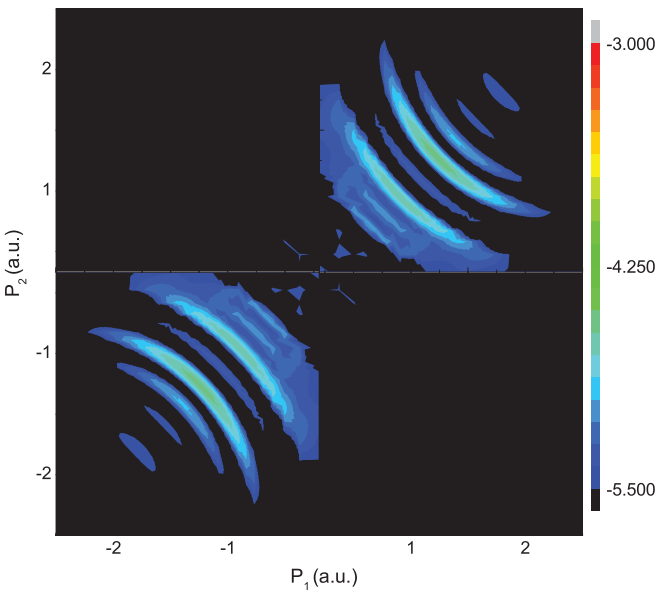

FIG. 1. (Color online) NSDI momentum spectra of two ionized electrons with their momenta parallel to the laser polarization direction. The laser intensity is 7×10^{14} W/cm^2, and the laser wavelength is 800 nm. In logarithmic scale.

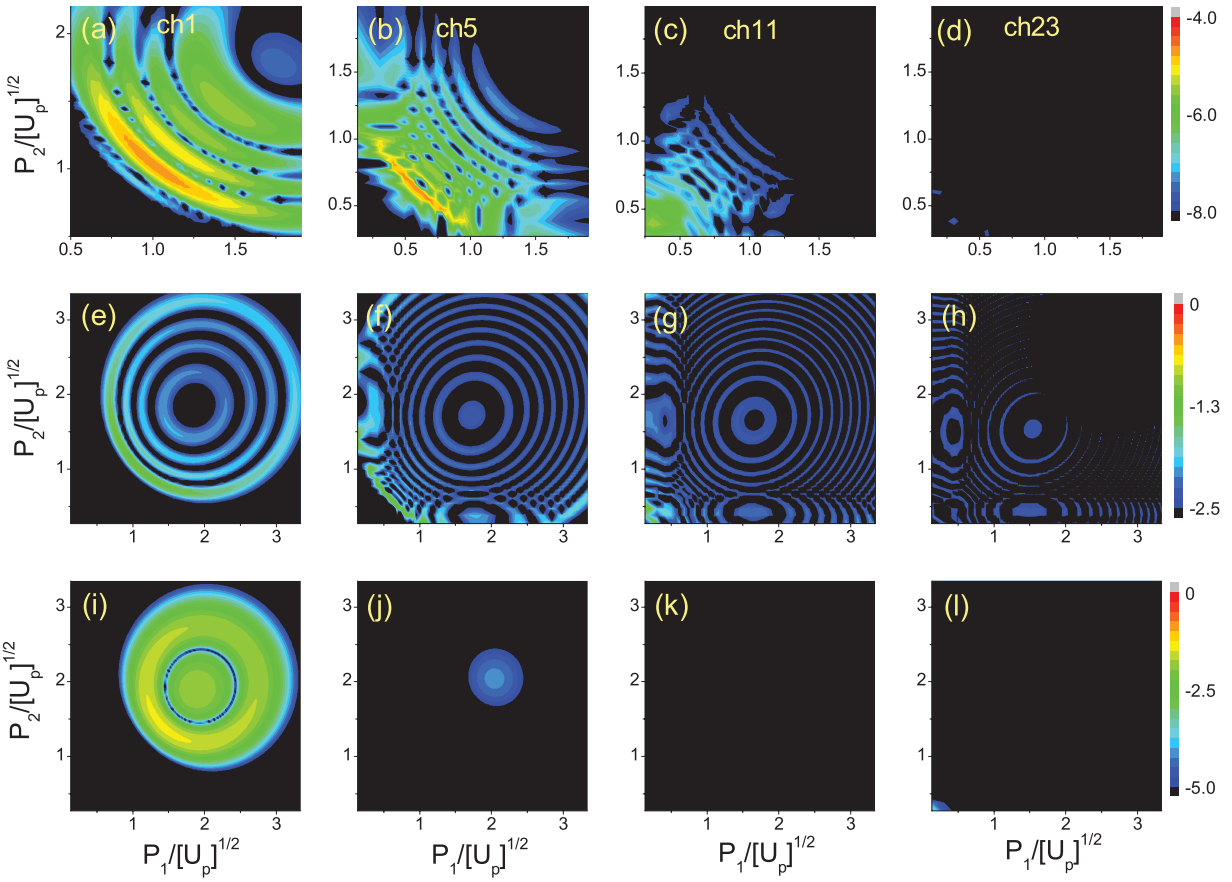

FIG. 2. (Color online) Channel contributions of NSDI momentum spectra with the final momenta of the two ionized electrons $\mathbf{p}_1$ and $\mathbf{p}_2$ along the $+z$ direction for (a) channel 1, (b) channel 5, (c) channel 11, and (d) channel 23. (e)–(h) present $|\mathcal{J}_{q_1+q_2-s}(\zeta,\eta)|^2$ for the backward collision for (e) channel 1, (f) channel 5, (g) channel 11, and (h) channel 23. (i)–(l) present $|\mathcal{J}_{q_1+q_2-s}(\zeta,\eta)|^2$ for the forward collision for (i) channel 1, (j) channel 5, (k) channel 11, and (l) channel 23. The laser intensity is 7×10^{14} W/cm^2. In logarithmic scale.

As we have mentioned above, the final result is obtained by summing up coherently the contributions of all ATI channels. From Eq. (21) we may find that the contribution from each ATI channel can be expressed as

$$T^k_{\rm CI}=\Gamma^k_{\rm LACI}\Gamma^k_{\rm ATI}\propto I(\mathcal{P})\mathcal{J}_{q_1+q_2-s}(\zeta_1+\zeta_2-\zeta_1',\eta)\Gamma^k_{\rm ATI}, \tag{25}$$

where $\Gamma^k_{\rm ATI}=V_e^{-1/2}\omega(u_p-s)\Phi_1(p_1')\mathcal{J}_s(\zeta_1',\eta)$ is the ATI amplitude for channel k, and $k=s-[\frac{E_1}{\omega}+u_p]$ is the order of the ATI channel. Clearly, one can see that the interference pattern comes from the LACI process $\Gamma^k_{\rm LACI}$. Particulary, it is from the generalized Bessel function $\mathcal{J}_{q_1+q_2-s}(\zeta_1+\zeta_2-\zeta_1',\eta)$ in Eq. (25). Therefore we should focus on analyzing this function in order to answer the above questions.

In general, the generalized Bessel function can be written as an integral form [13,27]:

$$\begin{aligned}&\mathcal{J}_{q_1+q_2-s}(\zeta_1+\zeta_2-\zeta_1',\eta)\\&=\frac{1}{2\pi}\int_{-\pi}^{\pi}d\varphi\exp\{i[(\zeta_1+\zeta_2-\zeta_1')\sin\varphi+\eta\sin2\varphi\\&\quad+(q_1+q_2-s)\varphi]\},\end{aligned} \tag{26}$$

where the argument $\zeta_1+\zeta_2-\zeta_1'=2\sqrt{u_p/\omega}(\mathbf{p}_1+\mathbf{p}_2-\mathbf{p}_1')\cdot\hat{\varepsilon}$, which depends on the direction of the momenta before and after the collision. Particularly, if the momentum $\mathbf{p}_1'$ is in the same direction of the momentum $\mathbf{p}_1$, we call this collision a forward collision; if these two momenta are in opposite directions, we call it a backward collision.

We now present the NSDI momentum spectra of the two electrons with their final momenta $\mathbf{p}_1$ and $\mathbf{p}_2$ along the $+z$ direction in Figs. 2(a)–2(d) for channels 1, 5, 11, and 23, respectively. From Figs. 2(a)–2(d), one can see that (1) the momentum distribution decreases as the channel order increases, which indicates that the lower channels dominate the contribution to the NSDI, and (2) the NSDI density distributes at larger momentum values for lower ATI channels and it distributes at lower momentum values for higher ATI channels. To explain these results, we present the momentum distribution of function $|\mathcal{J}_{q_1+q_2-s}(\zeta_1+\zeta_2-\zeta_1',\eta)|^2$ for a backward collision case, where $\mathbf{p}_1'$ is along the $-z$ direction, in Figs. 2(e)–2(h), as well as a forward collision case, where $\mathbf{p}_1'$ is along the $+z$ direction, in Figs. 2 (i)–2(l), for channel 1 [Figs. 2(e) and 2(i)], channel 5 [Figs. 2(f) and 2(j)], channel 11 [Figs. 2(g) and 2(k)], and channel 23 [Figs. 2(h) and 2(l)]. Comparing Figs. 2(a)–2(d) with 2(e)–2(h) and 2(i)–2(l), one can see that, for the case where the final momenta of two ionized electrons are in the same direction, the *backward collision* dominates the contribution to the NSDI, and the quantum interference pattern on the distribution of each channel shown in Figs. 2(a)–2(d)

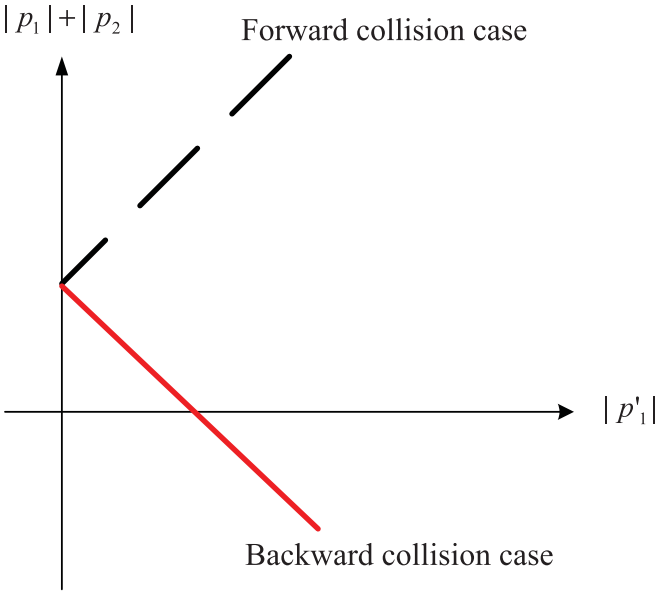

FIG. 3. (Color online) Schematic diagram showing the relationship between $|p_1|+|p_2|$ and $|p_1'|$ when f_1 is small. The dashed line is for the forward collision, and the solid line is for the backward collision.

is mainly determined by the characteristic of the backward collision of the corresponding channel.

In order to further understand the results shown in Fig. 2, we analyze the generalized Bessel function by using the classical action function $S_c(t,\mathbf{p}) = (1/2)\int dt[\mathbf{p} - e\mathbf{A}_c(t)]^2 = (\frac{\mathbf{p}^2}{2} + u_p\omega)t + \zeta\sin\omega t + \eta\sin 2\omega t$ [27]:

$$\mathcal{J}_{q_1+q_2-s}(\zeta_1+\zeta_2-\zeta_1',\eta) = \frac{\omega}{2\pi}\int_0^T dt\,\exp\{-i[\triangle S_c(t)+E_2 t]\}, \tag{27}$$

where $\triangle S_c(t) = S_c(t,\mathbf{p}_1) + S_c(t,\mathbf{p}_2) - S_c(t,\mathbf{p}_1')$ and $T = 2\pi/\omega$. Applying the saddle-point approximation, Eq. (27) becomes

$$\mathcal{J}_{q_1+q_2-s}(\zeta,\eta) = \frac{\omega}{2\pi}\sum_{t_0}\sqrt{\frac{2\pi}{i\triangle S_c''(t_0)}}\exp\{-i[\triangle S_c(t_0)+E_2 t_0]\}$$
$$= \frac{2\omega}{\pi\sqrt{\zeta\sin\omega t_0 + 4\eta\sin 2\omega t_0}}\cos\Theta, \tag{28}$$

where $\Theta = \zeta\sin\omega t_0 + \eta\sin 2\omega t_0 + (q_1+q_2-s)\omega t_0$ and $\zeta = \zeta_1+\zeta_2-\zeta_1'$. Here the saddle-point time t_0 satisfies the energy-conservation equation

$$\frac{[\mathbf{p}_1' - e\mathbf{A}_c(t_0)]^2}{2} - \frac{[\mathbf{p}_1 - e\mathbf{A}_c(t_0)]^2}{2} - \frac{[\mathbf{p}_2 - e\mathbf{A}_c(t_0)]^2}{2} = E_2, \tag{29}$$

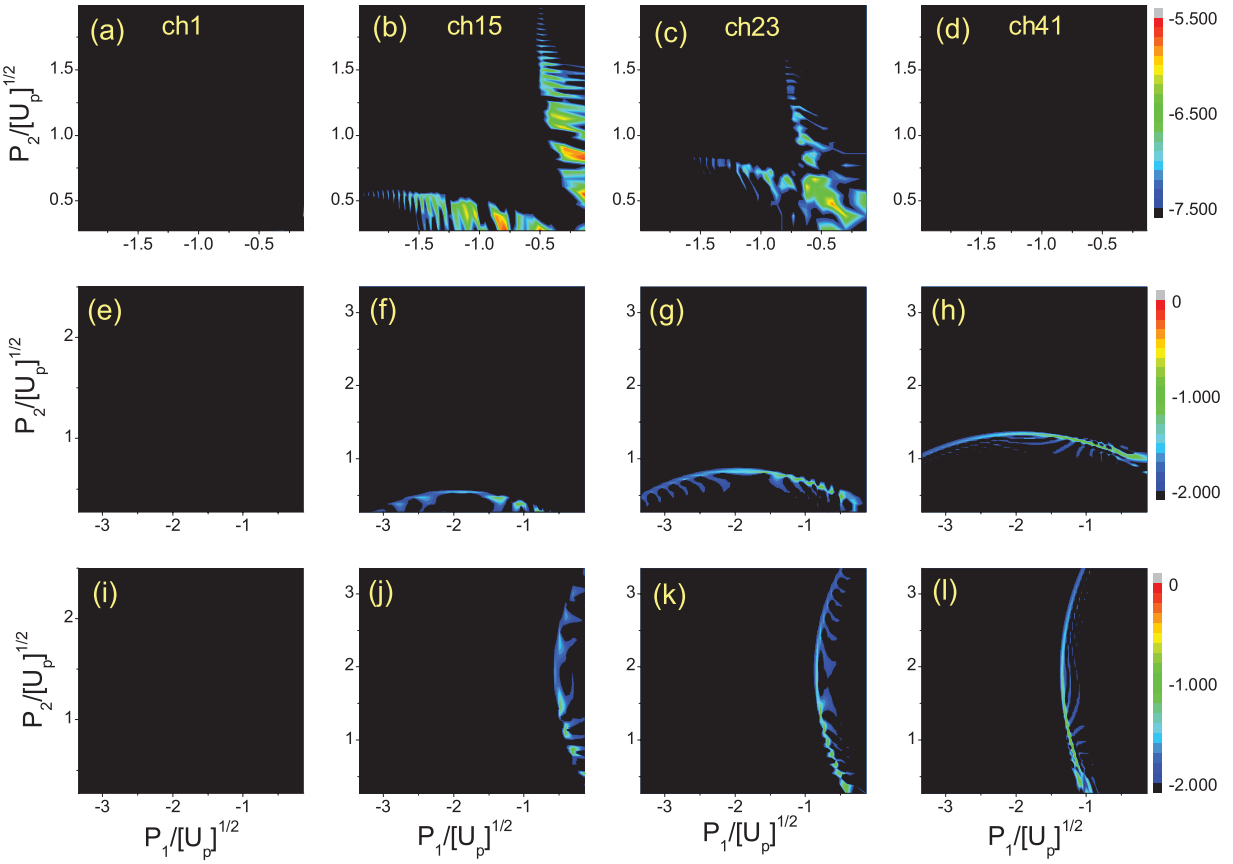

FIG. 4. (Color online) Channel contributions of NSDI momentum spectra of two ionized electrons with their momenta $\mathbf{p}_1$ along the $+z$ and $\mathbf{p}_2$ along the $-z$ directions for (a) channel 1, (b) channel 15, (c) channel 23, and (d) channel 41 (d). (e)–(h) present $|\mathcal{J}_{q_1+q_2-s}(\zeta,\eta)|^2$ for the backward collision for (e) channel 1, (f) channel 15, (g) channel 23, and (h) channel 41. (i)–(l) present $|\mathcal{J}_{q_1+q_2-s}(\zeta,\eta)|^2$ for the forward collision for (i) channel 1, (j) channel 15, (k) channel 23, and (l) channel 41. The laser intensity is 7×10^{14} W/cm^2. In logarithmic scale.

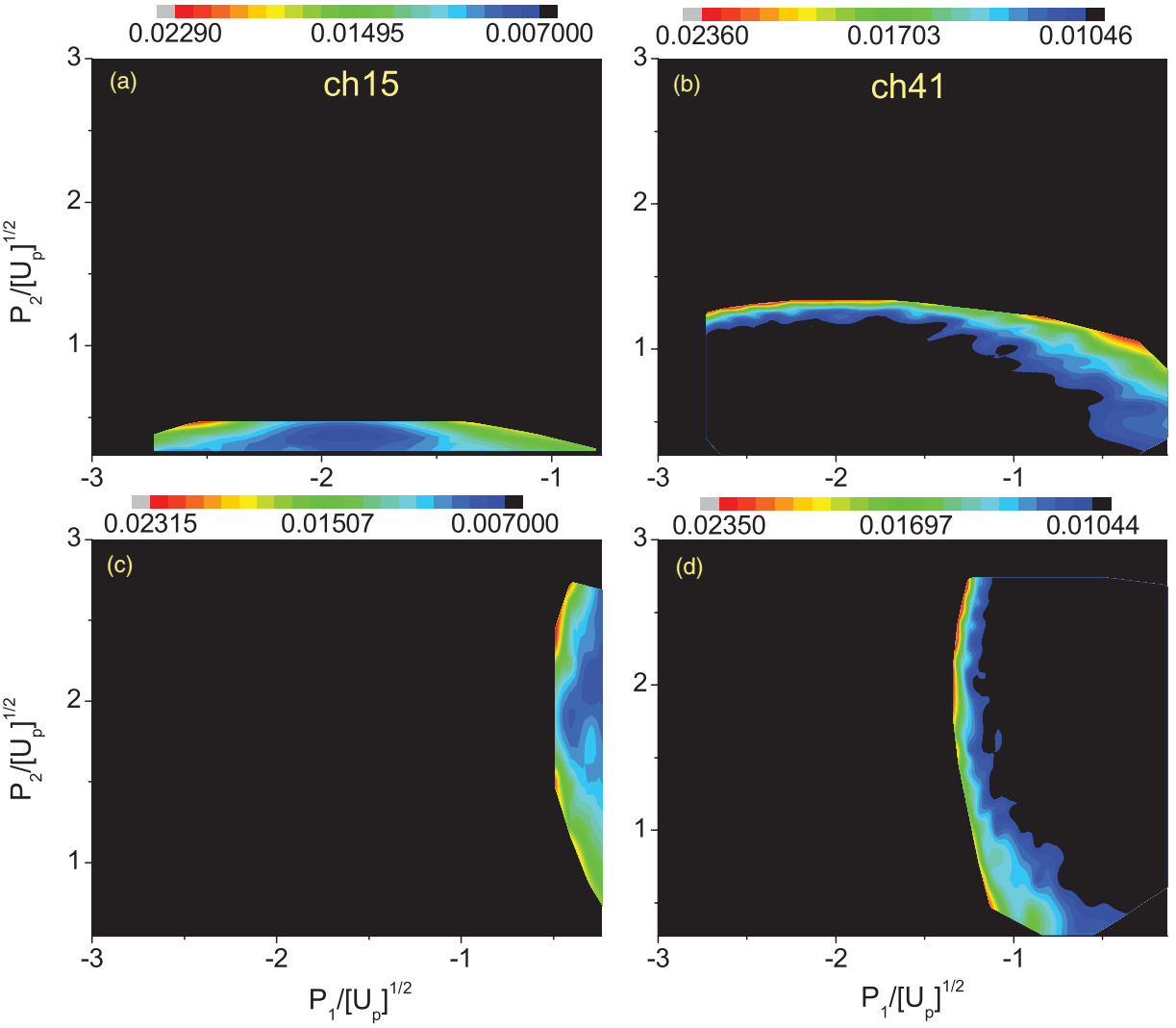

FIG. 5. (Color online) $|\mathcal{J}_{q_1+q_2-s}(\zeta,\eta)|^2$ calculated by using the saddle-point approximation as shown in Eq. (28) for the backward collision with (a) channel 15 and (b) channel 41and for the forward collision with (c) channel 15 and (d) channel 41.

i.e., $\zeta\cos(\omega t_0)+2\eta\cos(2\omega t_0)+(q_1+q_2-s)=0$. From Eq. (28) we find that the amplitude of the NSDI transition is proportional to $\sqrt{\frac{2\pi}{i\triangle S_c''(t_0)}}$, i.e., $\mathcal{J}_{q_1+q_2-s}(\zeta,\eta)\propto 1/\sqrt{f_1}$, where $f_1=-|p_1|-|p_2|-|p_1'|+2\sqrt{2\omega u_p}|\cos(\omega t_0)|$ for the backward collision and $f_1=-|p_1|-|p_2|+|p_1'|+2\sqrt{2\omega u_p}|\cos(\omega t_0)|$ for the forward collision. Obviously, the smaller the value of f_1 is, the larger the amplitude of $\mathcal{J}_{q_1+q_2-s}(\zeta,\eta)$ is. The relationship between $|p_1|+|p_2|$ and $|p_1'|$ for a fixed value of f_1 is depicted schematically in Fig. 3. As illustrated by Fig. 3, for the backward collision, the value of $|p_1|+|p_2|$ decreases as $|p_1'|$ increases, and hence the values of the momenta of the ionized electrons decrease as the channel order increases, as shown in Figs. 2(e)–2(h). On the contrary, for the case of forward collision, the value of $|p_1|+|p_2|$ increases with $|p_1'|$, and hence the values of the two momenta increase with the channel order, as shown in Figs. 2(i)–2(l). Furthermore, because higher values of the final momenta of the two electrons require more photon absorbtion during the ionization process, the NSDI probability will decrease as the final momenta of the two electrons increase. As a result, the backward collision plays a dominant role and the forward collision plays a less dominant role in an NSDI process.

On the other hand, the NSDI momentum spectra for the case where the two final momenta $\mathbf{p}_1$ and $\mathbf{p}_2$ are in *opposite* directions (i.e., $\mathbf{p}_1$ is in the $+z$ direction and $\mathbf{p}_2$ is in the $-z$ direction or vice versa), as shown in Fig. 1, can also be understood by analyzing Eq. (28). Figures 4(a)–4(d) show the NSDI momentum spectra of $\mathbf{p}_1$ along the $+z$ direction and $\mathbf{p}_2$ along the $-z$ direction for channels 1, 15, 23, and 41, respectively. One can see that (1) the low ATI channels cannot provide an obvious contribution to the NSDI but the middle ATI channels of order from about 15 to 35 make major contributions and (2) both the forward and backward collisions make equal contributions to the NSDI.

To explain these results, we first focus on the backward collision. The generalized Bessel function in Eq. (28) can also be expressed as $\mathcal{J}_{q_1+q_2-s}(\zeta,\eta)\propto 1/\sqrt{f_1}$, where f_1 now becomes $f_1=-|p_1|+|p_2|-|p_1'|+2\sqrt{2\omega u_p}|\cos(\omega t_0)|$. It is clear that the amplitude of the Bessel function becomes large when f_1 becomes small. Thus, if we set $f_1=0$,

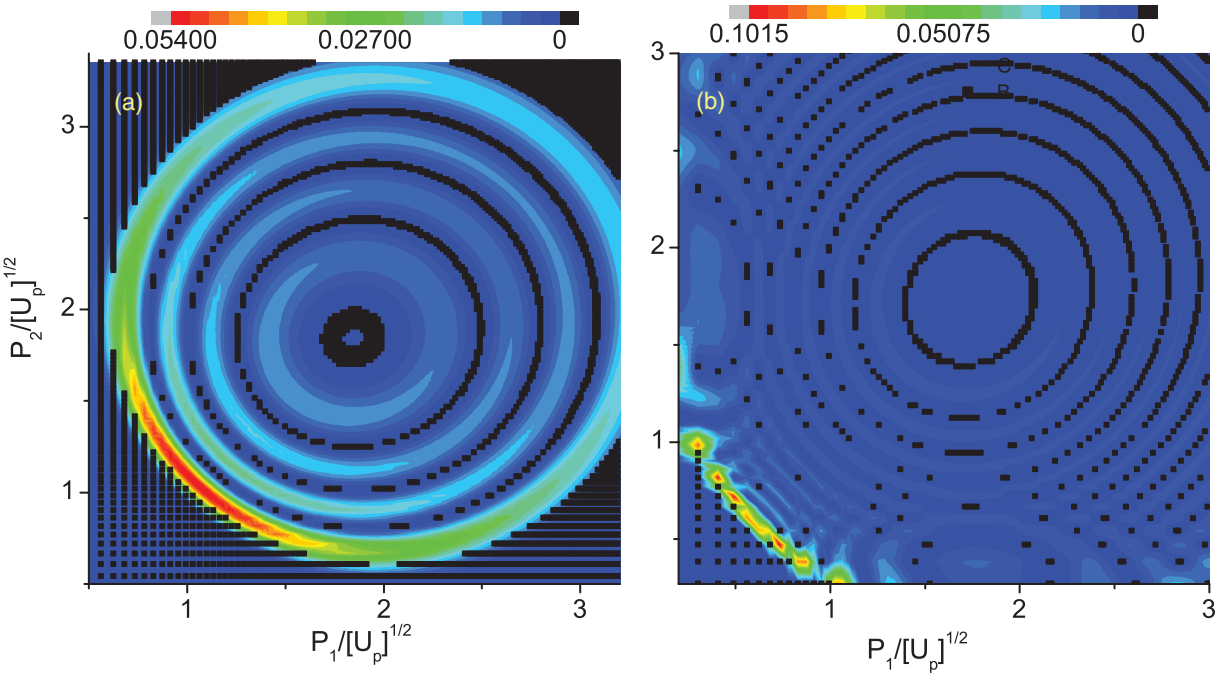

FIG. 6. (Color online) Interference fringes on the NSDI momentum distributions for (a) channel 1 and (b) channel 5. The solid squares show the positions where the function cos Θ equals zero.

$|p_1| = |p_2| - |p_1'| + 2\sqrt{2\omega u_p}|\cos(\omega t_0)|$. Hence for the low-channel case where $|p_1'| \approx 0$, $|p_1|$ has the minimum value of $2\sqrt{2\omega u_p}|\cos(\omega t_0)|$. Moreover, as the channel order increases, the value of $|p_1'|$ increases; hence the minimum value of $|p_1| = -|p_1'| + 2\sqrt{2\omega u_p}|\cos(\omega t_0)|$ decreases. Since the NSDI probability is small if the final kinetic energy of the ionized electron is large, the NSDI probability for low ATI channels is small, and it will increase with the ATI channel order. In our calculations, we found that the major contributions to the NSDI come from the ATI channels higher than 15. Furthermore, for the middle channels, in order for $|f_1|$ to be small, $|p_2|$ must remain small, as shown in Fig. 4(f); moreover, as the channel order increases, $|p_1'|$ becomes larger, and thus f_1 can be small even if $|p_2|$ increases, as shown in Figs. 4(f)–4(h). On the other hand, for the case of forward collision, the roles of $|p_1|$ and $|p_2|$ are exchanged, and the results shown in Figs. 4(j)–4(l) can be understood with a similar analysis. To confirm this investigation, Fig. 5 shows $|\mathcal{J}_{q_1+q_2-s}(\zeta,\eta)|^2$ using the saddle-point approximation for the backward [Figs. 5(a) and 5(b)] and forward [Figs. 5(c) and 5(d)] collisions for channel 15 [Figs. 5(a) and 5(c)] and channel 41 [Figs. 5(b) and 5(d)]. We can see that the results from the saddle-point approximation agree with the quantum numerical ones, as shown in Fig. 4.

We now investigate the source of the interference fringes appeared in Fig. 1. Because the final distribution shown in Fig. 1 comes from the coherent summation over all channel contributions, the interference lies in the NSDI density distribution for each ATI channel, as shown in Figs. 2(a)–2(d). From Eq. (28), we find that the interference comes from the function cos Θ, where the destructive interference lines should appear as $\cos\Theta = 0$, as shown by the dark squares in Figs. 6(a) and 6(b) for channels 1 and 5. One can see that the locations of these dark squares agree well with the distribution of minima from the quantum calculations, as shown in Fig. 6. From the saddle-point approximation, we may find that the interference fringes in Figs. 2(a)–2(d) come from the interference between the two trajectories that are born at the saddle-point time t_0 and $2\pi/\omega - t_0$, where the phase difference of these two trajectories leads to the cosine function. This result is similar to a HATI process of an atom or a molecule in a laser field [13,27].

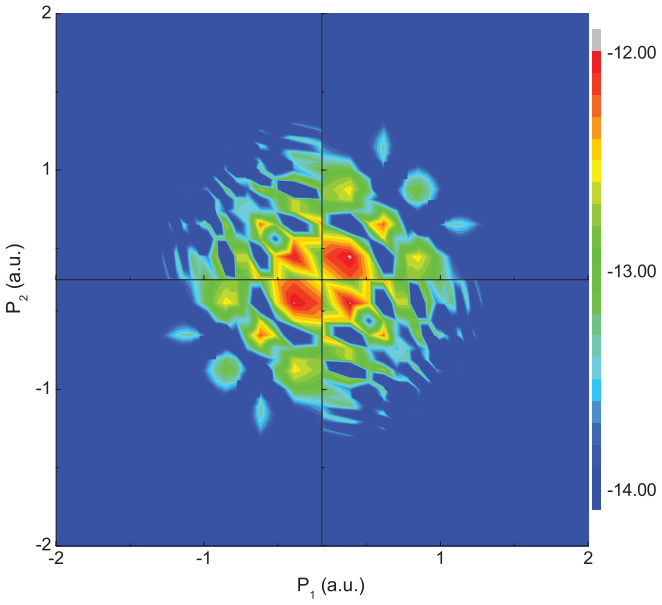

FIG. 7. (Color online) NSDI momentum spectra for the CEI mechanism with two ionized electrons momenta parallel to the laser polarization direction. The laser intensity is 2.2×10^{14} W/cm^2. In logarithmic scale.

IV. CEI PROCESSES IN NSDI

We now consider an NSDI of atomic helium dominated by the CEI mechanism, where the kinetic energy of the recollision electron is not large enough to ionize the bound electron directly by collision. Figure 7 presents the NSDI momentum spectra of helium with the momenta of the two ionized electrons along the laser's polarization direction. The laser intensity is 2.2×10^{14} W/cm^2, and the laser wavelength is 800 nm. We notice that our results shown in Fig. 7 agree qualitatively with the experimental results shown in Fig. 2(b) of Eremina *et al.* [35], where the corresponding perpendicular momenta have been integrated in their experiments. Comparing with Fig. 1, we may see that the NSDI probability for the final momenta of two electrons along the same direction is now comparable to that along the opposite directions. This result can be easily understood through Eq. (24), which can be rewritten as

$$T^k_{\rm CEI} = \Gamma^k_{\rm ATI2}\Gamma^k_{\rm LACE}\Gamma^k_{\rm ATI1} \propto I'(\mathcal{P})J_{q_1-s}(\zeta_1' - \zeta_1)\Gamma^k_{\rm ATI2}\Gamma^k_{\rm ATI1}, \tag{30}$$

where $\Gamma^k_{\rm ATI1}$ and $\Gamma^k_{\rm ATI2}$ are the ATI transition terms for the two electrons and $\Gamma^k_{\rm LACE} \propto I'(\mathcal{P})J_{q_1-s}(\zeta_1' - \zeta_1)$ represents the LACE transition. We can see that the probability for the LACE transition depends only on the momentum of the collision electron before and after it collides with the bound electron and is completely independent of the final momentum of the second electron, which is ionized by the laser from its excited state after the collision. As a result, Fig. 7 shows a symmetric structure with momenta $\mathbf{p}_1$ and $\mathbf{p}_2$.

Let us investigate the contributions from the forward and backward collisions due to the CEI mechanism. In calculating the CEI of helium, we found that the backward collision makes major contributions to the NSDI and the forward collision makes a negligible contribution, no mater which directions the two final momenta are. Figures 8(a)–8(d) present the NSDI momentum spectra of the two ionized electrons with their momenta along the laser's polarization direction for different channels. Figures 8(e)–8(h) show the NSDI momentum spectra for the backward collision. It is seen that, for the CEI mechanism, the NSDI momentum spectra of backward collision agree with the total NSDI momentum spectra for ATI channels, which confirms the above observation. This result can also be explained by analyzing the Bessel function $J_{q_1-s}(\zeta_1 - \zeta_1')$, which carries a crucial piece of information about the collision of the first ionized electron:

$$\begin{aligned} J_{q_1-s}(\zeta_1-\zeta_1') &= \frac{1}{2\pi}\int_{-\pi}^{\pi} d\theta \exp\{-i[(\zeta_1-\zeta_1')\sin\theta-(q_1-s)\theta]\} \\ &= \frac{\omega}{2\pi}\int_0^T dt \exp\{-i[\triangle S_c(t) + \triangle E_2 t]\}, \end{aligned} \tag{31}$$

where $\triangle S_c(t) = S_c(t,\mathbf{p}_1) - S_c(t,\mathbf{p}_1')$, $\triangle E_2$ is the energy difference between the ground state and the first excited state of He^+, and $T = 2\pi/\omega$. This expression indicates that the collision is an inelastic one, with the energy change being $\triangle E_2$. We may also use the saddle-point approximation to obtain the following expression for the Bessel function:

$$J_{q_1-s}(\zeta_1-\zeta_1') = \frac{\omega}{2\pi}\sum_{t_0}\sqrt{\frac{2\pi}{i\triangle S_c''(t_0)}}\exp\{-i[\triangle S_c(t_0)+\triangle E_2 t_0]\}, \tag{32}$$

where the saddle-point time t_0 now satisfies the equation [36]

$$\frac{[\mathbf{p}_1' - \mathbf{A}_c(t_0)]^2}{2} - \frac{[\mathbf{p}_1 - \mathbf{A}_c(t_0)]^2}{2} = \triangle E_2. \tag{33}$$

In the above, $\mathbf{A}_c(t_0)$ is the potential of the classical laser field. This expression is similar to the HATI process discussed in Ref. [27], where the only difference is that the HATI process is an elastic collision process. The interesting fact from our

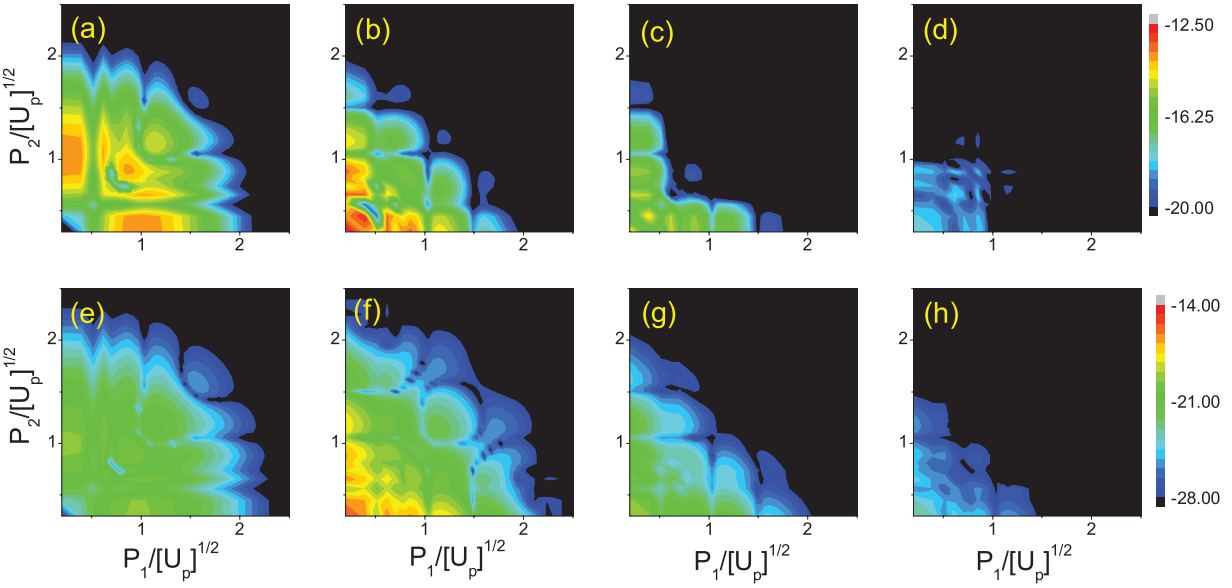

FIG. 8. (Color online) Channel contributions of NSDI momentum spectra for the CEI mechanism with two ionized electrons momenta parallel to the laser polarization direction for (a) channel 1, (b) channel 5, (c) channel 12, and (d) channel 20. (e)–(h) present the backward collision contributions to the CEI-NSDI. The laser intensity is 2.2×10^{14} W/cm^2. In logarithmic scale.

calculations is that, because of the large energy difference $\triangle E_2$ for atomic helium, the major contribution to the NSDI comes from quantum trajectories rather than classical ones, where the recollision time is imaginary, i.e., $t = (i/\omega)\cosh^{-1}(q_1 - s)/(\zeta_1 - \zeta_1')$. Thus the Bessel function becomes

$$J_L(\zeta_1 - \zeta_1') = \frac{\omega}{2\pi}\sum_{t_0}\sqrt{\frac{2\pi}{\omega^2[L^2 - (\zeta_1 - \zeta_1')^2]^{1/2}}} \times \exp\{-i[(\zeta_1 - \zeta_1')\sin(\omega t_0) - L\omega t_0]\}, \quad (34)$$

where $L = q_1 - s$ is the change of the photon number during the recollision. Similar to the CI case, the transition amplitude can be expressed as $T^k_{\mathrm{CEI}} \propto 1/f^{1/4}$, where f now is $f = L^2 - |\zeta_1 - \zeta_1'|^2 = L^2 - |\zeta_1|^2 - |\zeta_1'|^2 + |\zeta_1\zeta_1'|\cos\theta$, with θ being the phase difference between ζ_1 and ζ_1'. In particular, $\theta = 0$ is for the forward collision, and $\theta = 180^\circ$ is for the backward collision. Since L is large for large ΔE_2, f is always smaller for the case of backward collision than for the forward collision. This is the reason why the backward collision dominates in an NSDI process for the case of helium. On the other hand, one may find that if ΔE_2 is small, then the classical trajectories with real saddle-point times t_0 will play an important role in NSDI, and hence the forward collision may replace the role of the backward collision and dominate the contribution to NSDI.

V. CONCLUSIONS

Based on the strong-field nonperturbative quantum electrodynamics, we have developed the frequency-domain formalism for calculating the NSDI probabilities due to collision ionization and collision-excitation ionization mechanisms. By analyzing the contributions from each ATI channel, we have found that the backward collision plays a dominant role in both the CI and CEI processes in the NSDI for the case of atomic helium. Furthermore, we have also found that the quantum interference fringes in the NSDI momentum distributions for each ATI channel are attributable to the interference between two trajectories created at two different times.

ACKNOWLEDGMENTS

This research was supported by the National Natural Science Foundation of China under Grants No. 60778009, No. 11074296, and No. 11074026. Z.C.Y. was supported by NSERC of Canada. J.C. was also supported by the National Basic Research Program of China (Grant No. 2011CB8081002). B.W. thanks W. Becker, Xiaojun Liu, Jigen Chen, and Jiangbin Gong for helpful discussions and suggestions. This research was supported in part by the Project of Knowledge Innovation Program (PKIP) of the Chinese Academy of Sciences, Grant No. KJCX2.YW.W10.

[1] K. J. Schafer, B. Yang, L. F. DiMauro, and K. C. Kulander, Phys. Rev. Lett. **70**, 1599 (1993); P. B. Corkum, *ibid.* **71**, 1994 (1993).
[2] F. Krausz and M. Ivanov, Rev. Mod. Phys. **81**, 163 (2009).
[3] H. Niikura, H. J. Worner, D. M. Villeneuve, and P. B. Corkum, Phys. Rev. Lett. **107**, 093004 (2011).
[4] M. Hentschel *et al.*, Nature (London) **414**, 509 (2001).
[5] M. Fieb, B. Horvath, T. Wittmann, W. Helml, Y. Cheng, B. Zeng, Z. Xu, A. Scrinzi, J. Gagnon, F. Krausz, and R. Kienberger, New J. Phys. **13**, 033031 (2011).
[6] J. Itatani *et al.*, Nature (London) **432**, 867 (2004); S. Patchkovskii, Z. Zhao, T. Brabec, and D. M. Villeneuve, Phys. Rev. Lett. **97**, 123003 (2006).
[7] R. Torres, N. Kajumba, J. G. Underwood, J. S. Robinson, S. Baker, J. W. G. Tisch, R. de Nalda, W. A. Bryan, R. Velotta, C. Altucci, I. C. E. Turcu, and J. P. Marangos, Phys. Rev. Lett. **98**, 203007 (2007).
[8] H. J. Worner, H. Niikura, J. B. Bertrand, P. B. Corkum, and D. M. Villeneuve, Phys. Rev. Lett. **102**, 103901 (2009).
[9] D. Shafir, Y. Mairesse, D. M. Villeneuve, P. B. Corkum, and N. Dudovich, Nat. Phys. **5**, 412 (2009).
[10] Z. Zhai, J. Chen, Z.-C. Yan, P. Fu, and B. Wang, Phys. Rev. A **82**, 043422 (2010).
[11] A. A. Gonoskov, I. A. Gonoskov, M. Yu. Ryabikin, and A. M. Sergeev, Phys. Rev. A **77**, 033424 (2008).
[12] M. Busuladzic, A. Gazibegovic-Busuladzic, D. B. Milosevic, and W. Becker, Phys. Rev. Lett. **100**, 203003 (2008).
[13] Y. Guo, P. Fu, Z.-C. Yan, J. Gong, and B. Wang, Phys. Rev. A **80**, 063408 (2009).
[14] H. Kang, W. Quan, Y. Wang, Z. Lin, M. Wu, H. Liu, X. Liu, B. B. Wang, H. J. Liu, Y. Q. Gu, X. Y. Jia, J. Liu, J. Chen, and Y. Cheng, Phys. Rev. Lett. **104**, 203001 (2010).
[15] B. Wang, Y. Guo, B. Zhang, Z. Zhao, Z.-C. Yan, and P. Fu, Phys. Rev. A **82**, 043402 (2010).
[16] L. Holmegaard *et al.*, Nat. Phys. **6**, 428 (2010).
[17] A. l'Huillier, L. A. Lompre, G. Mainfray, and C. Manus, Phys. Rev. A **27**, 2503 (1983).
[18] R. Moshammer, B. Feuerstein, W. Schmitt, A. Dorn, C. D. Schroter, J. Ullrich, H. Rottke, C. Trump, M. Wittmann, G. Korn, K. Hoffmann, and W. Sandner, Phys. Rev. Lett. **84**, 447 (2000); Th. Weber, M. Weckenbrock, A. Staudte, L. Spielberger, O. Jagutzki, V. Mergel, F. Afaneh, G. Urbasch, M. Vollmer, H. Giessen, and R. Dörner, *ibid.* **84**, 443 (2000).
[19] A. Becker and F. H. M. Faisal, Phys. Rev. Lett. **89**, 193003 (2002).
[20] M. Weckenbrock, A. Becker, A. Staudte, S. Kammer, M. Smolarski, V. R. Bhardwaj, D. M. Rayner, D. M. Villeneuve, P. B. Corkum, and R. Dorner, Phys. Rev. Lett. **91**, 123004 (2003).
[21] J. Chen, J. Liu, L. B. Fu, and W. M. Zheng, Phys. Rev. A **63**, 011404(R) (2000); L. B. Fu, J. Liu, J. Chen, and S. G. Chen, *ibid.* **63**, 043416 (2001); L. B. Fu, J. Liu, and S. G. Chen, *ibid.* **65**, 021406(R) (2002); H. Li, J. Chen, H. Jiang, J. Liu, P. Fu, Q. Gong, Z.-C. Yan, and B. Wang, J. Phys. B **42**, 125601 (2009); H. Li, J. Chen, H. Jiang, P. Fu, J. Liu, Q. Gong, Z.-C. Yan, and B. Wang, Opt. Express **16**, 20562 (2008).
[22] C. Figueira de Morisson Faria and X. Liu, J. Mod. Opt. **58**, 1076 (2011).

[23] D.-S. Guo and T. Åberg, J. Phys. A **21**, 4577 (1988); D.-S. Guo and G. W. F. Drake, *ibid.* **25**, 3383 (1992).
[24] L. Gao, X. Li, P. Fu, R. R. Freeman, and D. S. Guo, Phys. Rev. A **61**, 063407 (2000).
[25] P. Fu, B. Wang, X. Li, and L. Gao, Phys. Rev. A **64**, 063401 (2001).
[26] T. Cheng, X. Li, S. Ao, L. A. Wu, and P. Fu, Phys. Rev. A **68**, 033411 (2003).
[27] B. Wang, L. Gao, X. Li, D. S. Guo, and P. Fu, Phys. Rev. A **75**, 063419 (2007).
[28] M. Gell-Mann and M. L. Goldberger, Phys. Rev. **91**, 398 (1953); M. L. Goldberger and K. M. Watson, *Collision Theory* (Wiley, New York, 1964).
[29] D.-S. Guo, T. Åberg, and B. Crasemann, Phys. Rev. A **40**, 4997 (1989).
[30] F. H. M. Faisal, Phys. Lett. A **187**, 180 (1994); A. Becker and F. H. M. Faisal, Phys. Rev. A **50**, 3256 (1994).
[31] A. Staudte, C. Ruiz, M. Schoffler, S. Schossler, D. Zeidler, Th. Weber, M. Meckel, D. M. Villeneuve, P. B. Corkum, A. Becker, and R. Dorner, Phys. Rev. Lett. **99**, 263002 (2007).
[32] A. Rudenko, V. L. B. de Jesus, Th. Ergler, K. Zrost, B. Feuerstein, C. D. Schroter, R. Moshammer, and J. Ullrich, Phys. Rev. Lett. **99**, 263003 (2007).
[33] C. Figueira de Morisson Faria, H. Schomerus, X. Liu, and W. Becker, Phys. Rev. A **69**, 043405 (2004).
[34] A. Becker and F. H. M. Faisal, J. Phys. B **29**, L197 (1996).
[35] E. Eremina, X. Liu, H. Rottke, W. Sandner, A. Dreischuh, F. Lindner, F. Grasbon, G. G. Paulus, H. Walther, R. Moshammer, B. Feuerstein, and J. Ullrich, J. Phys. B **36**, 3269 (2003).
[36] T. Shaaran, M. T. Nygren, and C. Figueira de Morisson Faria, Phys. Rev. A **81**, 063413 (2010).